Oligomerization affects the kinetics and thermodynamics of the interaction of a Bowman-Birk inhibitor with proteases.

Brand, G.D.[1,2*], Pires, D.A.T.[1,3], Furtado Jr., J.R.[4], Cooper, A.[5], Freitas, S.M.[6], Bloch Jr., C.[1]

[1] Laboratório de Espectrometria de Massa, EMBRAPA – Recursos Genéticos e Biotecnologia. Brasília, DF, Brasil;
[2] Laboratório de Síntese e Análise de Biomoléculas, Instituto de Química, Universidade de Brasília. Brasília, DF, Brasil;
[3] Instituto Federal de Educação, Ciência e Tecnologia de Goiás, Luziânia, GO, Brasil;
[4] Departamento de Polícia Federal, Unidade Técnico-Científica, Londrina, PR, Brasil;
[5] School of Chemistry, University of Glasgow, Glasgow G12 8QQ, Scotland, UK;
[6] Laboratório de Biofísica, Instituto de Biologia, Universidade de Brasília, Brasília, DF, Brasil;

Short title: BTCI oligomerization affects protein binding.

*Corresponding author: Guilherme Dotto Brand (gdbrand@unb.br)

Address: Instituto de Química, Campus Darcy Ribeiro, Universidade de Brasília (UnB), CEP 70910-900, Brasília, DF, Brasil. Phone: +55 61 3107 3857

Abbreviations: BTCI: black-eyed pea trypsin/chymotrypsin inhibitor; SPR: Surface Plasmon Resonance; ITC: Isothermal Titration Calorimetry; BBI: Bowman-Birk inhibitor; MUTMAC: 4-Methylunibelliferyl p-(NNN-trimethylaminonium)-cinnamate chloride; 4-MU: 4-methylumbelliferone.

Abstract

The black-eyed pea trypsin/chymotrypsin inhibitor (BTCI) forms concentration dependent homomultimers, as previously demonstrated by Light scattering and Atomic Force Microscopy. Considering that these self-aggregates might influence their binding to cognate enzymes, we investigated the interaction of BTCI at picomolar concentrations using surface immobilized Chymotrypsin (α-CT) and Trypsin (T) by Surface Plasmon Resonance. Our results indicate that BTCI has subnanomolar affinity to both immobilized enzymes, which is approximately two orders of magnitude higher than previously reported. Moreover, we probed the influence of temperature on protein binding equilibria in order to investigate their interaction energetics. While the BTCI/T interaction concurs with the canonical entropy-driven mechanism described for BBI interactions with serine proteinases, the BTCI/α-CT interaction does not. Our measurements indicate that bimolecular BTCI/α-CT complexes form with a negative enthalpy change and a moderate entropic increase. Direct calorimetric evaluation is in accord with the van´t Hoff approximation obtained by SPR. We demonstrate that as protein concentrations increase to the micromolar range, secondary endothermic events become prevalent and affect both the kinetics and thermodynamics of protein associations. Our study reinforces that BBI interactions with serine proteinases should be studied in dilute solutions to abridge often neglected secondary interactions.

Keywords: Surface plasmon resonance; protein interactions; BBI; Isothermal Titration Calorimetry; Protease Inhibitor.

1. Introduction

Bowman-Birk inhibitors (BBIs) and their interactions with proteolytic enzymes have been the subject of intense research since the first reports of enzyme activity depletion due to inhibitor complexation [1]. In dicotyledonous plants, BBIs are present as double-headed inhibitors having molecular masses ranging from 6 to 9 kDa, seven disulphide bonds, and two homologous and independent enzyme-specific binding loops [2]. Although it has been thoroughly reported that these molecules form simple bimolecular heterocomplexes with chymotrypsin (α-CT) and trypsin (T), the acquisition of accurate kinetic and thermodynamic parameters is challenging. Besides the specific interactions between inhibitory loops and enzyme active sites, secondary binding sites and self-aggregates have been described, which result in complex binding equilibria (3–5).

The black-eyed pea trypsin/chymotrypsin inhibitor (BTCI) is an 83-residue BBI (9.1 kDa) isolated from the seeds of *Vigna unguiculata* (c.v. Seridó) [6]. It presents rich biotechnological potential as an anticarcinogenic agent, as a guanylin-enhancing natriuresis and renal functional response in rats, as a bradykinin-potentiating molecule, and as an insecticide, inhibiting the growth of larvae with agricultural importance [7–12]. BTCI is composed mainly of anti-parallel beta-sheets containing reactive sites for T (Lys26) and α-CT (Phe53) in two independent canonical loops connected by the β-hairpin motif [13]. Moreover, it forms stable binary and tertiary complexes with T and α-CT presenting binding constants from 10^7 to 10^9 M^{-1} [14,15]. BTCI has an unusual solvent exposed hydrophobic patch with buried hydrophilic residues at subdomain 2, a characteristic feature of BBIs that is considered the source of their self-association

tendencies [13,16,17]. BTCI forms concentration dependent self-oligomers, ranging from monomers to dimers, trimers and hexamers as demonstrated by light scattering and atomic force microscopy [18,19].

The present work explores the kinetics and thermodynamics of the BTCI interaction with surface immobilized α-CT and T at physiological pH by Surface Plasmon Resonance (SPR). This technique monitors the formation and dissolution of protein complexes in nanomolar/picomolar concentrations, where BTCI is thought to be predominantly in monomeric form according to light scattering measurements [18]. Direct calorimetric evaluation by isothermal titration calorimetry (ITC) is performed to validate SPR thermodynamic data. According to our measurements, BTCI interacts with α-CT and T with higher affinity and with different interaction energetics than previously estimated [14,15]. To our best judgment, it is feasible to attribute the observed discrepancies in kinetic and thermodynamic constants between our data and previous assessments to be a result of numerous secondary concentration-dependant binding events.

2. Material and Methods

2.1. Proteins. α-CT from bovine pancreas was purchased from Serva Electrophoresis GmBh (Heidelberg, Germany) and used without further purification. Sequencing grade modified T from Promega (Madison, WI, USA) was used due to pronounced autolysis observed in preliminary tests with unmodified trypsin, which precluded data acquisition (data not shown). Methylated T is referred plainly as T throughout the whole manuscript. BTCI was purified from the seeds of *Vigna unguiculata* as previously described [6].

Protein concentrations were determined by spectrophotometry (Shimadzu, Tokyo, Japan) according to previously published works [13].

2.2. Surface plasmon resonance and isothermal titration calorimetry. BTCI interactions with surface-immobilized serine proteinases were evaluated in a BIACORE 3000 (GE Healthcare, Buckinghamshire, UK) biosensor. HBS-EP buffer, CM5 sensor chips, amine coupling kits and immobilization and regeneration buffers were purchased from GE Healthcare. A MicroCal VP-ITC (GE Healthcare, Buckinghamshire, UK) was used to evaluate the BTCI/α-CT interaction in solution. Filtered and degassed HBS-E buffer (10 mM HEPES, pH 7.4, 150 mM NaCl, 3mM EDTA) was used for calorimetric evaluations.

2.3. α-CT and T sensor chip immobilization. CM5 sensor chips were docked and hydrated for about 24 hours before protein immobilization. T and α-CT were immobilized by standard amine coupling using HBS-EP as running buffer. Both serine proteinases were individually resuspended in acetate buffer pH 5.5 at a concentration of $5\mu g.mL^{-1}$ and injected in the flow cells activated with NHS/EDC until the desired immobilization levels were attained (approximately 700 RU for α-CT and 1200 for T). Experimental and control cells were deactivated with 1M Ethanolamine. Lysine-methylated T was probably immobilized in its free N-terminus using standard amine coupling chemistry.

2.4. BTCI interaction analyses with α-CT and T by SPR. SPR analyses were performed at a 50 $\mu L.min^{-1}$ flow rate. Regeneration conditions consisted in one 30s injection of 10 mM glycine buffer pH 2.4 for the BTCI/T interaction, and two injections for the BTCI/α-CT interaction. BTCI was dissolved in HBS-EP buffer in serial two-fold

dilutions, from 250 to 3.9 nmoles.L^{-1}. Concentration series were injected over surface immobilized enzymes. Each concentration series consisted of BTCI injected twice at each concentration at each evaluated temperature (15 to 35°C in 5° intervals). Data corresponding to the association phase of interactions were acquired for 4 min, and the dissociation phase was monitored for 25 min due to the slow dissociation kinetics. Bulk refractive index changes were corrected using a reference flow cell and double reference buffer injections were performed. Sensorgrams were fit to a simple bimolecular model (A + B ↔ AB) using BIAevaluation 3.1. Global data fittings were performed for each concentration series.

2.5. Thermodynamic analysis of SPR binding data. Equilibrium kinetics data for the BTCI/α-CT and BTCI/T interactions were fit to the non-linear form of the Gibbs-Helmholtz equation [20] using Origin 7.0 (Origin Lab, MA, USA).

$$\Delta G^{\circ} = \Delta H_o - T\Delta S_o + \Delta C_p(T - T_0) - T(\Delta C_p.\ln(\frac{T}{T_0})) \qquad (1)$$

Transition state analysis was carried out using the Eyring equations, which assume an active state in equilibrium with reactants (A + B ↔AB* ↔ AB) whose concentration determines the velocity of the reaction [21]. This should be considered simply as a convenient semi-empirical model in the current context.

2.6. Isothermal titration calorimetry. BTCI was submitted to 3 cycles of buffer exchange with HBS-E using Amicon 10 kDa centrifugal filters (Milipore, MA, USA), quantified and stored at -80 ºC until use. The enzyme α-CT was prepared fresh just before titrations and submitted to 3 cycles of buffer exchange with HBS-E before protein quantification by spectrophotometry [13]. The operational molarity of α-CT after buffer exchange was estimated using a spectrofluorimetric method [22]. Briefly, a 5-fold molar

excess of MUTMAC was incubated with α-CT in HBS-E buffer for 10 min following the quantification of 4-MU compared to a 1 nmole.L^{-1} standard solution. Spectrofluorimetric measurements were performed in octuplicates on a Spectramax M2 instrument (Molecular Devices, CA, USA). Microcalorimetric reaction cells were filled with BTCI and titrated with α-CT; Protein concentrations are indicated in each experiment. Syringe rotor speed was set to 300 rpm and 28 α-CT injections were performed, 10 μL each, following standard instrument procedures. α-CT dilution heats were determined in independent experiments and subtracted from the titration data. The BTCI/T interaction could not be evaluated due to trypsin autolysis, and the methylated T was not used due to high sample requirements. Calorimetric data were obtained and evaluated using the Origin software 7.0 (Origin Lab, MA, USA).

3. Results

3.1. BTCI has subnanomolar affinity to α-CT and T.

The BTCI interaction kinetics with α-CT and T was evaluated by SPR at nanomolar concentrations from 15 to 35ºC. The enzymes α-CT and T, the latter derivatized by reductive methylation, were immobilized on the dextran surface of CM5 sensor chips using standard amine coupling chemistry. Mass transport effects were considered negligible at 50 μL/min, and the linked reaction test detected no obvious intermediate state for both reactions (data not shown). Binding curves resulting from the injection of 250 to 3.9 nmol.L^{-1} BTCI over surface-immobilized α-CT and T were fit to a simple bimolecular interaction model at the evaluated temperatures. Sensorgrams and their corresponding fittings (in red) are displayed in Figure 1. Data for the BTCI/T interaction

presented higher deviations from the model, possibly due to residual enzyme autolysis [1]. BTCI both associates and dissociates with T twice as fast as it does with α-CT at 25°C, but both inhibitor/enzyme complexes present undistinguishable equilibrium binding affinities (Table 1). Indeed, the equilibrium dissociation constants (K_D) of the BTCI/α-CT and BTCI/T complexes at 25ºC are 0.41 ± 0.00 and 0.42 ± 0.07 nM, respectively. Temperature had opposite effects on the stability of protein complexes: while the BTCI/α-CT affinity decreased nearly three times as the reaction temperature shifted from 15 to 35 ºC, the formation of the BTCI/T complex was favored roughly by the same amount (Table 1).

3.2. BTCI interacts with α-CT and T with distinct thermodynamic profiles.

SPR derived equilibrium dissociation constants were used to calculate the Gibbs free energy of binding (ΔG) of the BTCI/α-CT and BTCI/T complexes and the Gibbs-Helmholtz equation was fit to the data (Eq. 1). A linear dependency was observed between the ΔG and reaction temperature for the BTCI/T interaction, indicating a negligible heat capacity change (ΔCp_{vh}) upon complex formation (Figure 2). On the other hand, the complexation between BTCI and α-CT occurred with a negative ΔCp_{vh}, as it is observed in other protein-protein interactions (Table 2) [23]. While the formation of the BTCI/α-CT complex is exothermic and favored by an entropy increase ($\Delta H°_{vh}$ = -7.5 ± 0.9 kcal.mol^{-1} and $\Delta S°_{vh}$= 18 ± 3 cal.mol^{-1}.K^{-1}), the BTCI/T interaction is endothermic and therefore driven by a large entropy increase ($\Delta H°_{vh}$= 8 ± 2 kcal.mol^{-1} and $\Delta S°_{vh}$= 70 ± 6 cal.mol^{-1}.K^{-1}). Eyring equations were used to dissect the reaction pathways by

introducing a theoretical transient state (Figure 2A and 2B) [21]. Theoretical reaction pathways were built based on transition state theory and they are depicted in Figure 3.

3. 3. BTCI interaction with α-CT in solution by ITC.

Considering that the BTCI/α-CT thermodynamics described herein contradicts previously published data [14], we sought to validate results by direct thermodynamic measurements. For such, the BBI was loaded in the ITC microcalorimeter cell at 3μM and titrated at 25ºC with α-CT at 20μM, in HBS-E buffer, pH 7.4. The operational molarity of α-CT following sample preparation was 94 ± 3%, indicating that the enzyme remains competent after buffer exchange. The steepness of the binding curve in the titration isotherm prevented an accurate estimation the association constant (K_A) for these proteins by ITC, therefore the kinetic parameters obtained by SPR were used. The measured BTCI/α-CT enthalpy and entropy of interaction at 25ºC were $\Delta H°_{cal}$ = -7.0 ± 0.1 kcal.mol^{-1} and $\Delta S°_{cal}$ = 19 cal.mol^{-1}.K^{-1} (Figure 4). Increasing the BTCI concentration in the reaction cell to 5 μM introduced non-negligible endothermic events following the association between the inhibitor and the enzyme (Figure 4B). Further six-fold increase in BTCI concentration (Figure 4C) introduced significant post-active site titration endothermic events, producing a complex titration data. At the concentration of 30 μM, the association between BTCI and α-CT active sites was followed by more significant endothermic events. Moreover, the reaction stoichiometry shifted from 1:~2 to 1:~4 α-CT:BTCI as BTCI concentrations increased from 3 to 30μM in the reaction cell (Figure 4A to 4C).

4. Discussion

The present work reports the kinetics and thermodynamics of the interaction between BTCI, a double-headed BBI, with the serine proteinases α-CT and T by SPR. Dilute protein solutions were used as an effort to abridge the concentration-dependant multiple linked chemical equilibria that are characteristic to BBI interactions with serine proteinases [4]. The agreement between SPR sensorgrams and the bimolecular model observed in Figure 1 indicates that simple protein associations occurred in this experimental setup, without appreciable parallel reactions (Table 1, Figure 1). SPR data specifies that, at nanomolar concentrations, BTCI has an undistinguishable affinity to both surface-immobilized enzymes (Table 1). The K_D of the BTCI interaction with α-CT and T were previously estimated as 1.15×10^{-7} M and 6.25×10^{-9} M at 298K, respectively [14,15]. Data obtained by SPR represents approximately a 300-fold higher affinity for α-CT and a 15-fold higher affinity for T than previously assessed by indirect assays using samples at micromolar concentrations [14,15]. We propose that BTCI multimers, which become more prevalent with increasing protein concentration, constitute less or even unreactive inhibitor species by hindering the enzyme access to the inhibitor enzyme-binding loops, as previously indicated by AFM data [13]. Evaluation of the BTCI molecule X-ray structure suggest that the α-CT binding loop should indeed be more influenced by protein aggregation, in accordance with our observations. The BTCI α-CT binding loop (Phe53) is encoded within the subdomain 2 region, recognized as the hydrophobic core that drives BBI multimerization [13]. Further evidence is obtained by AFM with the detection of an unreactive BTCI fraction following the inhibitor incubation

with equimolar amounts of α-CT, while only bimolecular complexes are detected after its incubation with T [13].

Distinct thermodynamic profiles were obtained for the BTCI interaction with α-CT and T by SPR at 25ºC (Table 2, Figure 3). While the BTCI/T interaction is endothermic and driven by entropy, which concurs with previously obtained data [15,24], the BTCI/α-CT interaction is exothermic, in disagreement with previous assays [14]. The ITC data in Figure 4 sheds light in these discrepancies. Previous BTCI/α-CT thermodynamic analyses were conducted with a minimum BTCI concentration of 6.2 µM [14], a concentration where secondary binding events, characterized by endothermic peaks, were detected by ITC (Figure 4B). Indeed, at 30 µM these endothermic events become not only detectable, but constitute the main source of heat exchange in the titration of BTCI with α-CT (Figure 4C). We cannot, at present, define the specific molecular events that result in such endothermic heat exchanges. However, we hypothesize that they are related to the dissolution of pre-formed BTCI self-aggregates and/or α-CT dimers [25], in an event that precedes the formation of specific enzyme/inhibitor complexes. Further experiments will be conducted to investigate such hypotheses. Moreover, unreactive BTCI self-aggregates can also explain the disparities in the reaction stoichiometry measured by SPR and ITC experiments. While the first detects only bimolecular complexes (Table 1), the latter shows a concentration dependent reaction stoichiometry (Figure 4A-C). Possible explanations reside in the SPR inherent insensitivity to pre-formed unreactive BTCI molecular species, which, if present at the assayed concentrations, are flowed-through the chip surface without producing measurable changes in refractive index.

The present paper demonstrates that BTCI forms simple bimolecular complexes with T and α-CT with similar affinity but distinct thermodynamic profiles when probed by Surface Plasmon Resonance. Moreover, the stoichiometry, kinetics and thermodynamics of the BTCI complexation with α-CT are consistently influenced by the increment in protein concentrations from the nanomolar to the micromolar range [13,14,26]. Our study indicates that secondary interactions should play an important role in the kinetic and thermodynamic parameters in protein interactions in certain experimental setups. Moreover, it reinforces that BBI interactions with serine proteinases should be studied in dilute solutions to abridge secondary interactions, which are often overlooked in biophysical investigations, and are much closer to the actual physiological scenario of these proteins.

5. Acknowledgments

The authors wish to dedicate this work to Dr. Manuel Mateus Ventura, for his pioneering work in the Biophysical evaluation of protein interactions. They also wish to express their gratitude to Mrs. Margareth Nutley for her scientific support. The authors received finacial support from Coordenação de Aperfeiçoamento de Pessoal de Nível Superior (CAPES), Conselho Nacional de Desenvolvimento Cientifico e Tecnológico (CNPq), Fundação de Amparo à Pesquisa do Distrito Federal (FAP-DF) and Financiadora de Estudos e Projetos (FINEP).

6. References

[1] M.J. Laskowski, R.W. Sealock, Protein Proteinase Inhibitors - Molecular Aspects. In The Enzymes., III, Academic Press, New York, 1971.

[2] K.N. Rao, C.G. Suresh, Bowman-Birk protease inhibitor from the seeds of Vigna unguiculata forms a highly stable dimeric structure., Biochim. Biophys. Acta. 1774 (2007) 1264–73. doi:10.1016/j.bbapap.2007.07.009.

[3] M.J. Gilleland, M.L. Bender, Kinetics of a-Chymotrypsin Dimerization, J. Biol. Chem. 251 (1976) 498–502.

[4] L.S. Gennis, Double-headed protease inhibitors from black-eyed peas. V. Analysis of the energetics of protease-inhibitor interactions., J. Biol. Chem. 251 (1976) 763–768.

[5] È. Koepke, U. Ermler, E. Warkentin, G. Wenzl, P. Flecker, Crystal Structure of Cancer Chemopreventive Bowman-Birk Inhibitor in Ternary Complex with Ê Resolution . Structural Basis Bovine Trypsin at 2 . 3 A of Janus-faced Serine Protease Inhibitor Specificity, J. Mol. Biol. 298 (2000) 477–491. doi:10.1006/jmbi.2000.3677.

[6] M.M. Ventura, J. Xavier Filho, A Trypsin and Chymotrypsin Inhibitor from Black-Eyed Pea (Vigna sinesis L.) I. Purification and Partial Characterization., An. Acad. Bras. Cienc. 38 (1966) 553–566.

[7] O.L. Franco, R.C. dos Santos, J.A.N. Batista, A.C.M. Mendes, M.A.M. de Araújo, R.G. Monnerat, et al., Effects of black-eyed pea trypsin/chymotrypsin inhibitor on proteolytic activity and on development of Anthonomus grandis., Phytochemistry. 63 (2003) 343–9. http://www.ncbi.nlm.nih.gov/pubmed/12737983 (accessed April 10, 2015).

[8] A. da Cunha Morales Álvares, E.F. Schwartz, N.O. Amaral, N.R. Trindade, G.R. Pedrino, L.P. Silva, et al., Bowman-Birk protease inhibitor from Vigna unguiculata seeds enhances the action of bradykinin-related peptides., Molecules. 19 (2014) 17536–58. doi:10.3390/molecules191117536.

[9] L. da C. Souza, R. Camargo, M. Demasi, J.M. Santana, C.M. de Sá, S.M. de Freitas, Effects of an anticarcinogenic Bowman-Birk protease inhibitor on purified 20S proteasome and MCF-7 breast cancer cells., PLoS One. 9 (2014) e86600. doi:10.1371/journal.pone.0086600.

[10] A. Carvalho, M. Santos-Neto, H. Monteiro, S. Freitas, L. Morhy, N. Nascimento, et al., BTCI enhances guanylin-induced natriuresis and promotes renal glomerular and tubular effects, Brazilian J. Biol. 68 (2008) 149–154. doi:10.1590/S1519-69842008000100021.

[11] A. Mehdad, G. Brumana, A. Souza, J. Barbosa, M. Ventura, S. de Freitas, et al., A Bowman–Birk inhibitor induces apoptosis in human breast adenocarcinoma through mitochondrial impairment and oxidative damage following proteasome 20S inhibition, Cell Death Discov. 2 (2016) 15067. doi:10.1038/cddiscovery.2015.67.

[12] G.A. Joanitti, R.B. Azevedo, S.M. Freitas, D.M. Parkin, F. Bray, J. Ferlay, et al., Apoptosis and lysosome membrane permeabilization induction on breast cancer cells by an anticarcinogenic Bowman-Birk protease inhibitor from Vigna unguiculata seeds., Cancer Lett. 293 (2010) 73–81. doi:10.1016/j.canlet.2009.12.017.

[13] A.R.G. Barbosa, L.P. Silva, R.C.L. Teles, G.F. Esteves, R.B. Azevedo, M.M. Ventura, et al., Crystal Structure of the Bowman-Birk Inhibitor from Vigna unguiculata ˚ Resolution and Its Structural Seeds in Complex with b -Trypsin at 1 . 55 A Properties in Association with Proteinases, Biophys. J. 92 (2007) 1638–1650. doi:10.1529/biophysj.106.090555.

[14] S.M. de Freitas, H. Ikemoto, M.M. Ventura, Thermodynamics of the binding of chymotrypsin with the black-eyed pea trypsin and chymotrypsin inhibitor (BTCI)., J. Protein Chem. 18 (1999) 307–13.

[15] H.C.. Fachetti, K. Mizuta, M.M. Ventura, Thermodynamics of the Association of Trypsin with the Black-Eyed Pea Trypsin and Chymotrypsin inhibitor, An. Acad. Bras. Cienc. 56 (1984) 311–317.

[16] P. Kumar, a G.A. Rao, S. Hariharaputran, N. Chandra, L.R. Gowda, Molecular mechanism of dimerization of Bowman-Birk inhibitors. Pivotal role of ASP76 in the dimerzation., J. Biol. Chem. 279 (2004) 30425–32. doi:10.1074/jbc.M402972200.

[17] R.H. Voss, U. Ermler, L.O. Essen, G. Wenzl, Y.M. Kim, P. Flecker, Crystal structure of the bifunctional soybean Bowman-Birk inhibitor at 0.28-nm resolution. Structural peculiarities in a folded protein conformation., Eur. J. Biochem. 242 (1996) 122–31. http://www.ncbi.nlm.nih.gov/pubmed/8954162.

[18] M.M. Ventura, K. Mizuta, H. Ikemoto, Self-association of the black-eyed pea trypsin and chymotrypsin inhibitor in solution - a study by light scattering, An. Acad. Bras. Cienc. 53 (1981) 195–201.

[19] L.P. Silva, R.B. Azevedo, P.C. Morais, M.M. Ventura, S.M. Freitas, Oligomerization states of Bowman-Birk inhibitor by atomic force microscopy and computational approaches., Proteins. 61 (2005) 642–8. doi:10.1002/prot.20646.

[20] N.V. Prabhu, K.A. Sharp, Heat Capacity in Proteins, Annu. Rev. Phys. Chem. 56 (2005) 521–548. doi:10.1146/annurev.physchem.56.092503.141202.

[21] Y.S.N. Day, C.L. Baird, R.L. Rich, D.G. Myszka, Direct comparison of binding equilibrium, thermodynamic, and rate constants determined by surface- and solution-based biophysical methods, Protein Sci. 11 (2002) 1017–1025.

[22] G.W. Jameson, D. V Roberts, R.W. Adams, W.S. Kyle, D.T. Elmore, Determination of the operational molarity of solutions of bovine alpha-chymotrypsin, trypsin, thrombin and factor Xa by spectrofluorimetric titration., Biochem. J. 131 (1973) 107–17. http://www.ncbi.nlm.nih.gov/pubmed/4737291 (accessed January 16, 2017).

[23] J.M. Sturtevant, Heat capacity and entropy changes in processes involving proteins, Proc. Natl. Acad. Sci. 74 (1977) 2236–2240.

[24] R.J. Baugh, C.G. Trowbridge, Calorimetry of Some Trypsin-Trypsin Inhibitor Reactions, Biol. Chem. 247 (1972) 7498–7501.

[25] R. Filfil, T. V. Chalikian, The thermodynamics of protein-protein recognition as characterized by a combination of volumetric and calorimetric techniques: The binding of Turkey ovomucoid third domain to ??-chymotrypsin, J. Mol. Biol. 326

(2003) 1271–1288. doi:10.1016/S0022-2836(03)00022-6.

[26] L.D.C. Souza, R. Camargo, M. Demasi, J.M. Santana, C.M. De Sá, S.M. De Freitas, Effects of an anticarcinogenic bowman-birk protease inhibitor on purified 20S proteasome and MCF-7 breast cancer cells, PLoS One. 9 (2014) 1–10. doi:10.1371/journal.pone.0086600.

Table 1. Kinetic parameters of the BTCI/α-CT and BTCI/T interactions as a function of temperature. Data are presented as mean ± standard deviation for 2 independent concentration series, each concentration injected in duplicate.

	BTCI:α-CT			**BTCI:T**		
Temp (K)	**$k_a \times 10^4$ $M^{-1}.s^{-1}$**	**$k_d \times 10^{-5}$ s^{-1}**	**$K_D \times 10^{-10}$ M**	**$k_a \times 10^4$ $M^{-1}.s^{-1}$**	**$k_d \times 10^{-5}$ s^{-1}**	**$K_D \times 10^{-10}$ M**
288	6.3 ± 0.4	2.4 ± 0.1	3.83 ± 0.00	11 ± 1	10 ± 2	9.6 ± 0.9
293	8.57 ± 0.04	3.1 ± 0.5	3.6 ± 0.6	19.2 ± 0.1	11.7 ± 0.5	6 ± 2
298	11.3 ± 0.03	4.6 ± 0.1	4.07 ± 0.04	21 ± 3	9 ± 1	4.2 ± 0.7
303	15.6 ± 0.1	9.5 ± 0.8	6 ± 1	44 ± 6	18 ± 6	4.0 ± 0.7
308	17.70 ± 0.02	14.6 ± 0.2	8 ± 1	44.05 ± 0.05	16.0 ± 0.8	4 ± 2

Table 2. Thermodynamics aspects of the formation of the BTCI/α-CT and BTCI/T complexes.

	BTCI/α-CT	**BTCI/T**
Gibbs-Helmholtz		
ΔG (kcal.mol^{-1})*	-12.76 ± 0.01	-12.74 ± 0.09
ΔH (kcal.mol^{-1})	-7.5 ± 0.9	8 ± 2
ΔS (cal.mol^{-1}.K^{-1})	18 ± 3	70 ± 6
ΔCp_{VH} (kcal.mol^{-1}.K^{-1})	-1.0 ± 0.3	
Transition State Theory		
ΔH_a (kcal.mol^{-1})	8.8 ± 0.6	12 ± 2
ΔH_d (kcal.mol^{-1})	16 ± 2	4 ± 3
ΔS_a (cal.mol^{-1}.K^{-1})	-6 ± 2	8 ± 7
ΔS_d (cal.mol^{-1}.K^{-1})	-24 ± 6	-63 ± 9

* ΔG obtained from $-RT\ln(K_A)$.

Figure Legends

Figure 1. Temperature dependence of the BTCI binding to surface-immobilized α-CT and T by Surface Plasmon Resonance. Black lines correspond to the binding responses obtained by the injection of a concentration series of BTCI, ranging from 250 to 3.9 nM, over α-CT (Left column) and T (Right column) derivatized dextran sensor chips at the temperatures shown at the sensorgrams. Red lines correspond to data fittings obtained by the adjustment to the simple bimolecular model (A+B ↔ AB).

Figure 2. Gibbs free energy of binding of the BTCI/α-CT and /T complexes and the temperature dependence of rate constants. Equilibrium dissociation constants obtained for the BTCI/α-CT (▲) and /T **(**■) interactions were used for the calculation of the Gibbs free energy of binding as a function of temperature. Data were fit to a non-linear form of the Gibbs-Helmholtz equation (red line) resulting in the thermodynamic parameters listed in Table 2. Insets A and B correspond to the Eyring plots generated for k_a and k_d for BTCI/α-CT (▲) and /T **(**■). Pearson correlation coefficients were higher than 0.95, except for the k_d of the BTCI/T complex (R = 0.65). Each data point is the average of duplicates and error bars correspond to standard deviation.

Figure 3. Energy profiles for the BTCI interaction with serine proteinases at pH 7.4. Theoretical minimum reaction paths for the BTCI/α-CT (▲) and /T **(**■) interactions.

Plots demonstrate ΔG^o, ΔH^o and $-T\Delta S^o$. Continuous red lines are used as a guide to the eye.

Figure 4. Calorimetric data for the interaction of BTCI with α-CT with varying protein concentrations. Raw data and integrated calorimetric traces for the injection 28 × 10 µL A) 20 µM α-CT into 3 µM BTCI, B) 50 µM α-CT into 5 µM BTCI and C) 200 µM α-CT into 30 µM BTCI. Raw data of control α-CT injections in HBS-E buffer are depicted above BTCI-α-CT calorimetric traces.

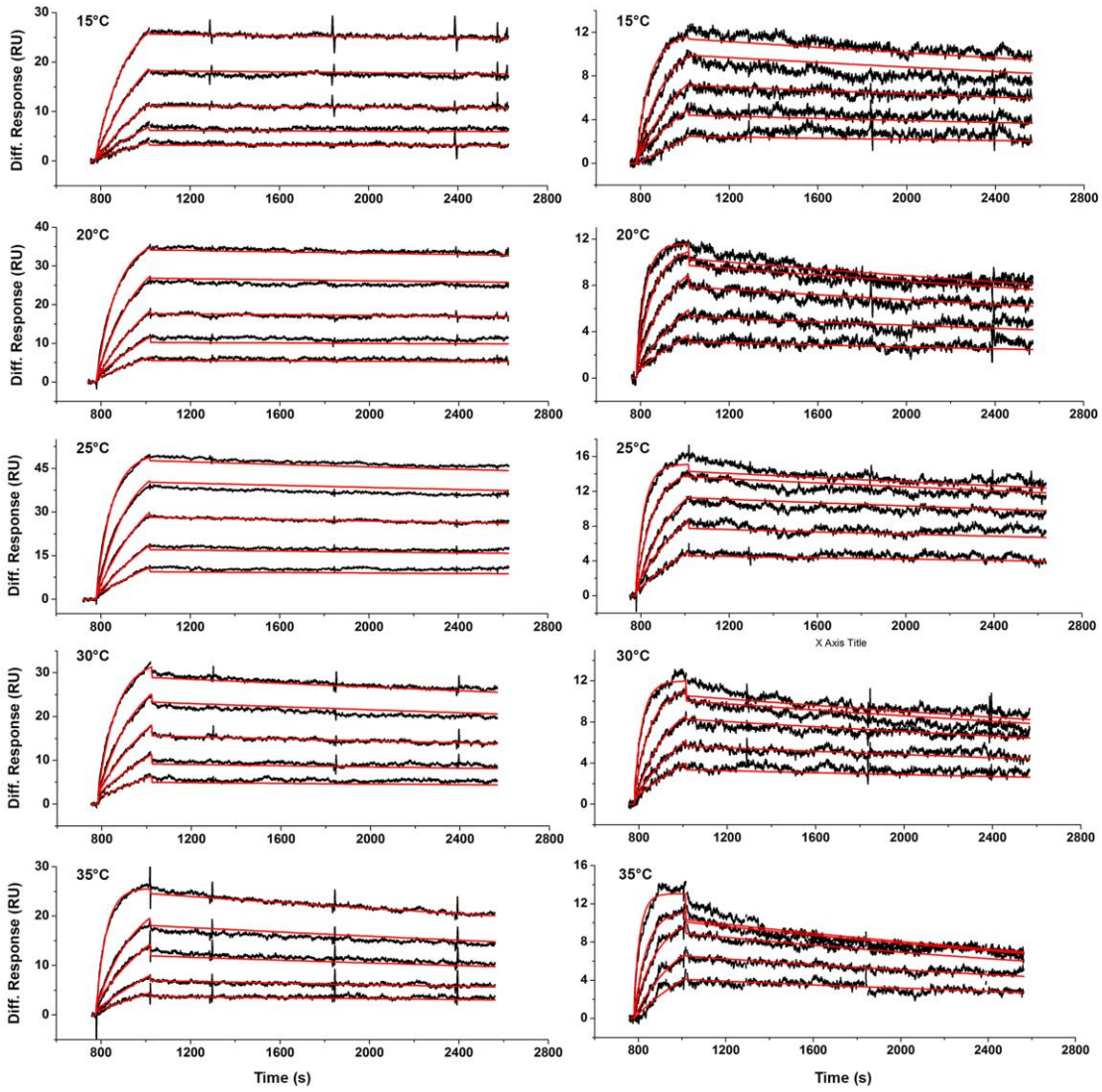

Figure 1

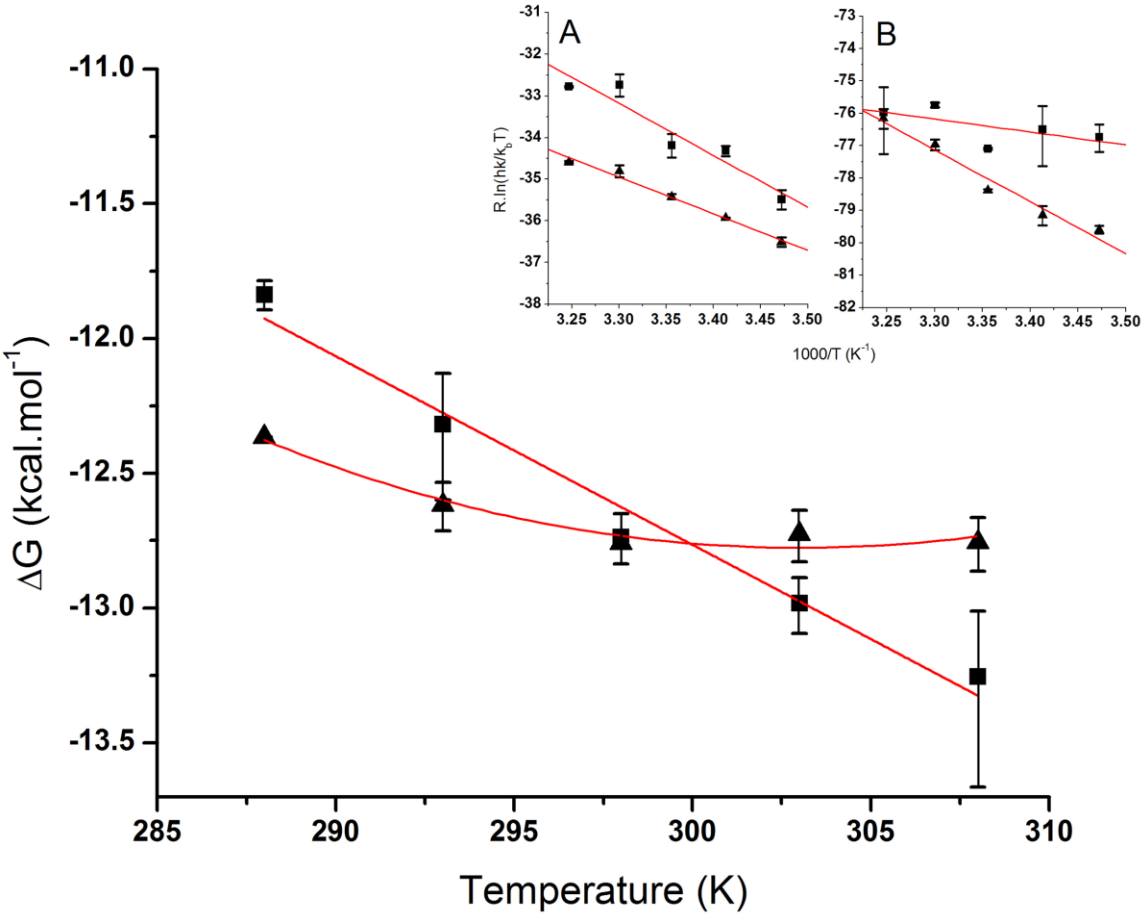

Figure 2

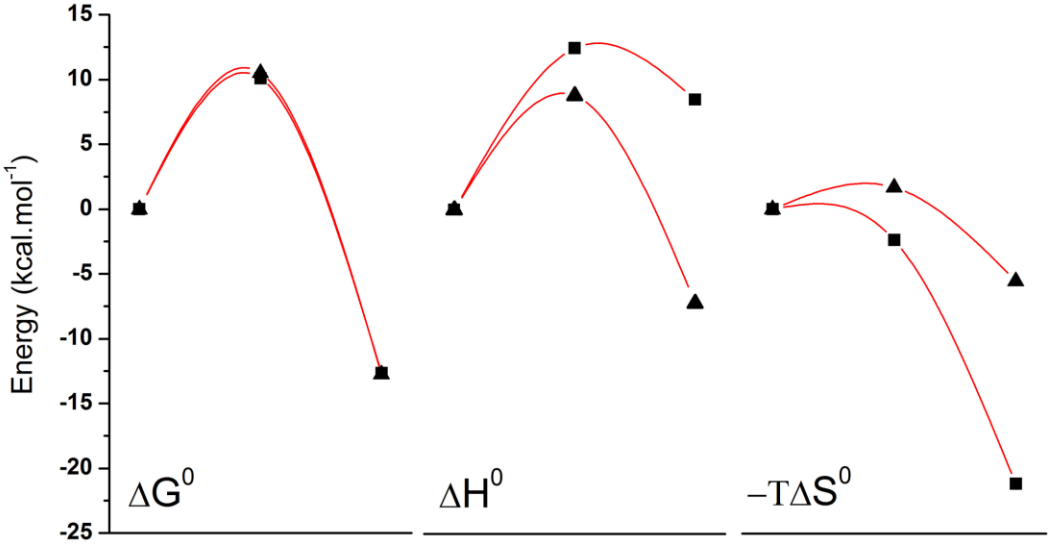

Figure 3

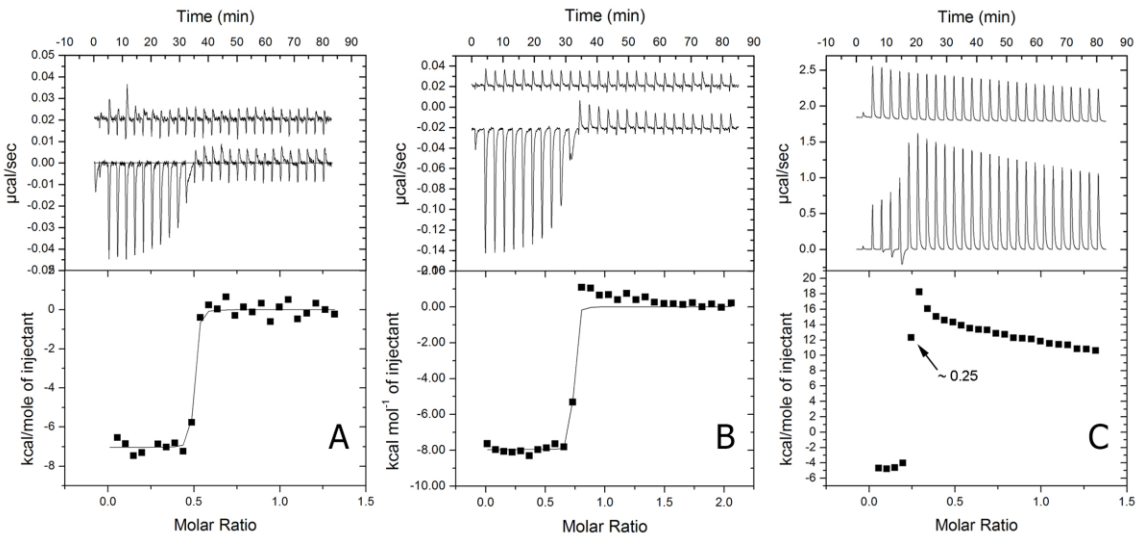
Time (min)
µcal/sec
kcal/mole of injectant
Molar Ratio
A
Time (min)
µcal/sec
kcal mol-1 of injectant
Molar Ratio
B
Time (min)
µcal/sec
kcal/mole of injectant
~ 0.25
Molar Ratio
C

Figure 4